Improvement in the anti-tumor efficacy of doxorubicin nanosponges in *in vitro* and in mice bearing breast tumor models

Benedetta Ferrara[a], Roberta Cavalli[a], Casimiro Luca Gigliotti[b], Nausicaa Clemente[b], Monica Argenziano[a], Elena Boggio[b], Annalisa Chiocchetti[b], Francesco Trotta[c], Mirella Giovarelli[d], Stefania Pizzimenti[e], Giuseppina Barrera[e], Renzo Boldorini[b], Roberto Fantozzi[a], Umberto Dianzani[b,], Chiara Dianzani[a]

[a] Dept. of Drug Science and Technology, University of Torino, Torino, Italy, [b] Interdisciplinary Research Center of Autoimmune Diseases (IRCAD) and Department of Health Sciences, UPO, Novara, Italy, [c] Dept. of Chemistry, University of Torino, Torino, Italy, [d]Dept. of Molecular Biotechnology and Health Sciences, University of Torino, Torino, Italy, [e] Dept. of Clinical and Biological Sciences, University of Torino, Orbassano, Torino, Italy

Doxorubicin (DOX) is an anthracycline widely used in cancer therapy and in particular for breast cancer treatment. Multidrug resistance (MDR) is one of the major unsolved problems regarding several anticancer drugs included DOX. However, high doses of DOX required to overcome MDR can induce severe nonspecific side effects, in particular cardiotoxicity, leading to several limitations in clinical application. A delivery system of DOX may overcome these disadvantages. Cyclodextrins (CD) are cyclic α-1,4-glucans that can be composed in a three-demensional network forming CD nanosponges (CD-NS), a novel nanosized delivery system able to incorporate a wide range of hydrophobic molecules. This work has the aim to evaluate the effects of a new formulation of DOX based on *β*-CD-NS containing the drug (BNS-DOX)*.

*BNS were synthesized by Prof. Trotta, *Dept. of Chemistry, University of Torino,* and DOX incorporated inside BNS by Prof. Cavalli, *Dept. of Drug Science and Technology, University of Torino.*

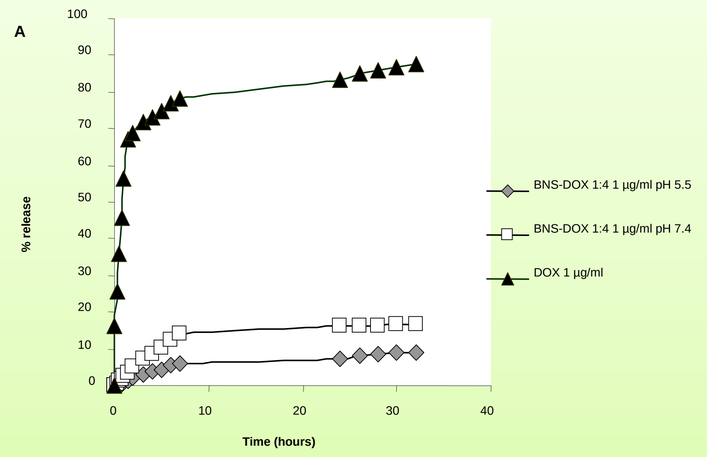

Figure 1: Kinetics of release profiles of DOX from BNS formulation at different pH values. A DOX solution is reported for comparison (**A**). TEM image of DOX-loaded BNS (**B**).

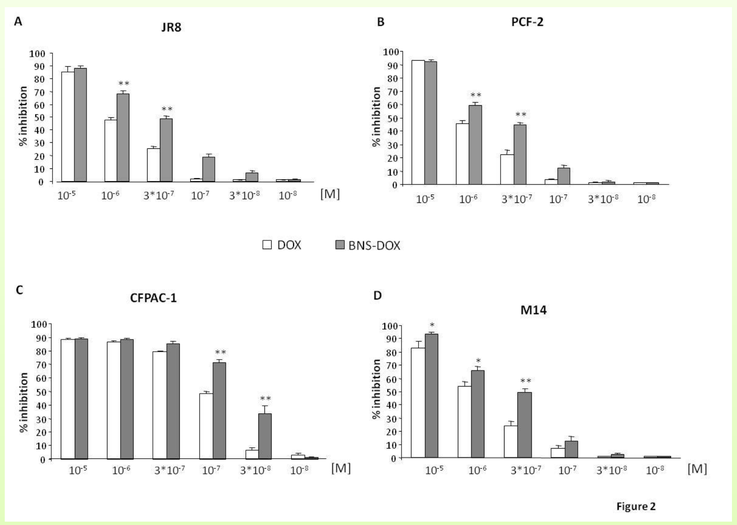

Figure 2: Percentage of cell survival following DOX and BNS-DOX treatment. Human melanoma cell lines JR8, PCF-2, M14, and human pancreas cancer cell line CFPAC-1 were treated with increasing concentrations of the drugs for h. The results are expressed as % of cell survival control and shown as mean ± SEM (*n* = 5). Eight replicate wells were used to determine each data point, and five different experiments were performed. ** p< 0.01, significantly different from CPT; one-way ANOVA and Dunnett's test.

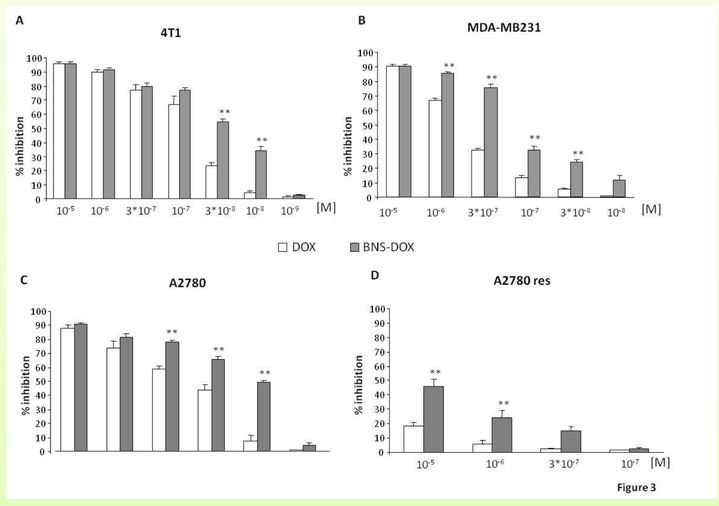

Figure 3: Percentage of cell survival following DOX and BNS-DOX treatment. Mouse (4T1) and Human (MDA-MB231) breast cancer cell line and ovarian cancer cell line (A2780 and A2780 DOX resistent) were treated with increasing concentrations of the drugs for h. The results are expressed as % of cell survival control and shown as mean ± SEM (*n* = 5). Eight replicate wells were used to determine each data point, and five different experiments were performed. ** p< 0.01, significantly different from CPT; one-way ANOVA and Dunnett's test.

Table 1: **IC_{50} of BNS-DOX and DOX on several cell lines**

Cell Line	IC_{50} BNS-DOX	IC_{50} DOX	P value
JR8	$2.86 \pm 0.33 \times 10^{-7}$	$8.8 \pm 1.4 \times 10^{-7}$	0.014
PCF2	$4.54 \pm 0.48 \times 10^{-7}$	$11.64 \pm 0.97 \times 10^{-7}$	0.0012
M14	$3.44 \pm 0.47 \times 10^{-7}$	$7.1 \pm 1 \times 10^{-7}$	0.021
A2780	$1.5 \pm 0.27 \times 10^{-9}$	$86.2 \pm 1.4 \times 10^{-9}$	0.0038
A2780res	$2 \pm 0.67 \times 10^{-5}$	$13.5 \pm 3.7 \times 10^{-5}$	0.038
CFPAC-1	$5.6 \pm 0.5 \times 10^{-8}$	$11.7 \pm 0.3 \times 10^{-8}$	0.001
MDA-MB231	$1.6 \pm 0.2 \times 10^{-7}$	$5 \pm 0.2 \times 10^{-7}$	0.001
4T1	$2.8 \pm 0.2 \times 10^{-8}$	$8.64 \pm 0.8 \times 10^{-8}$	0.0021

Two tailed P value has been determined with unpaired T test with Welch correction

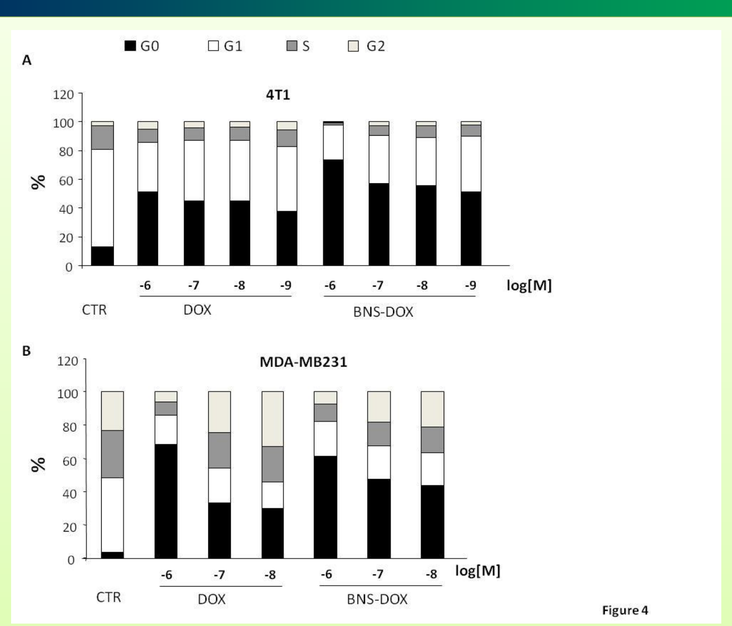

Figure 4: Effects of DOX and BNS-DOX treatment on cell cycle. 4T1 (**A**) and MDA-MB231 (**B**) cells (1.5×10^5) were treated or not with DOX and BNS-DOX for 72 h and the cell cycle was then assessed by flow cytometry. Graphs represented the % of the quantification of cell cycle phases from 3 independent experiments.

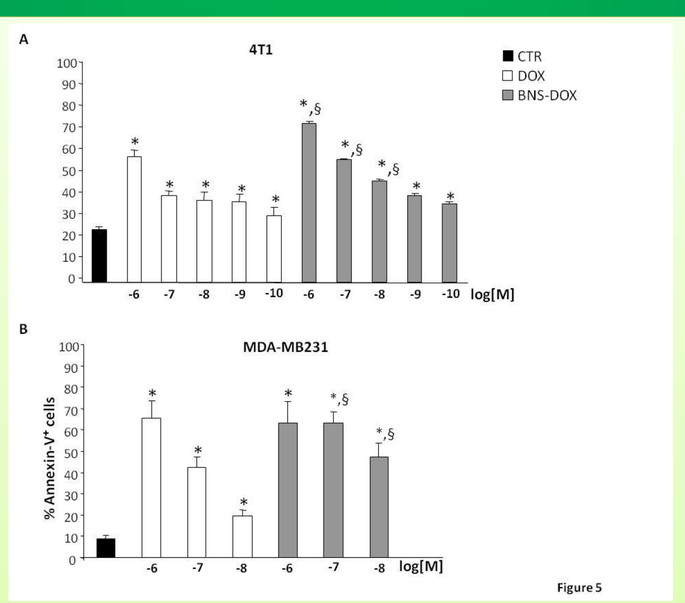

Figure 5: Effects of DOX and BNS-DOX treatment on cell death. Annexin-V positive cells were evaluated in 4T1 (**A**) and MDA-MB231 (**B**) cultured for 72 h in the presence or absence of DOX or BNS-DOX. Results are expressed as % of positive calculated as follows: (result displayed by each treatment / the results displayed by untreated cells) from 5 independent experiments (*p< 0.05, versus the control; § p< 0.05, versus the same concentration).

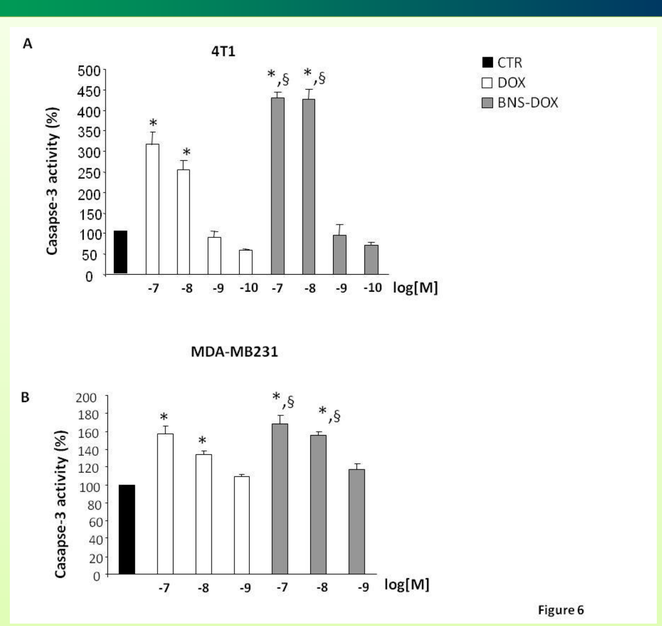

Figure 6: Levels of caspase-3 activity DOX and BNS-DOX treatment. Caspase-3 activity was evaluated in 4T1 (**A**) and MDA-MB231 (**B**) cultured for 72 h in the presence or absence of DOX or BNS-DOX. Results are expressed as described in Fig. 3 from 5 independent experiments (*p< 0.05, versus the control; § p< 0.05, versus the same concentration).

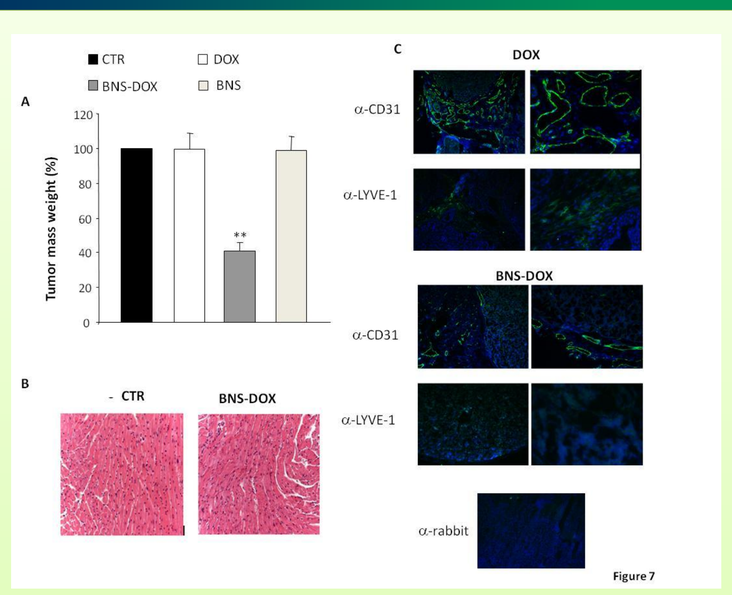

Figure 7: Effect of DOX and BNS-DOX on tumor growth in vivo. (**A**) The graph shows an average of the tumor mass weight, expressed as % compared to the control group, at time of sacrifice. (**B)** Histopathologic analysis of the heart. H&E stained were observed with 20X magnification. Representative image of heart tissue from Neu-T mice treated with PBS or BNS-DOX. Similar pictures were observed in mice treated with BNS or DOX. **(C)** Immunofluorescence staining of CD-31 and LYVE-1 of tumour tissue sections from of Neu-T mice treated with DOX or BNS-DOX. The slides were stained with either pAb rabbit α-mouse CD31 or pAb rabbit α-mouse LYVE-1 plus a secondary antibody α-rabbit conjugated with Alexa Fluor® 488.

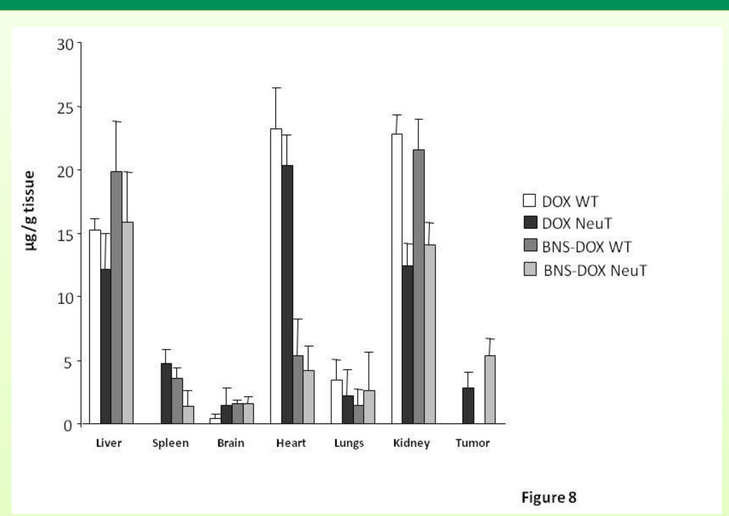

Figure 8. BNS-DOX displayed a significant higher distribution in the tumor site compared to free DOX in NeuT mice. A significant difference has been revealed also in the heart tissue, where BNS-DOX showed a strongly lower distribution than free DOX in NeuT and WT mice.*

*****In vivo* experiments were performed at the animal house of University of Novara (UPO) under the supervision of Prof. Umberto Dianzani, *Interdisciplinary Research Center of Autoimmune Diseases (IRCAD) and Department of Health Sciences, UPO.*

BNS-DOX significantly inhibits proliferation of several cancer cell lines, inhibits cell cycle progression and induces apoptosis of breast cancer cell lines in comparison with free DOX, as demonstrated by caspase 3 activity and annexin-V positive cells evaluation. Finally, BNS-DOX substantially delays the growth of breast cancer in BALB-neuT mice at a dose lower than the therapeutic one of DOX, reducing tumor neoangiogenesis and lymphangiogenesis. Biodistribution studies revealed a higher distribution in the tumor site and a lower distribution in the heart tissue compared with free DOX. This study shows that the use of BNS may be an efficient strategy for the delivery of DOX reducing its side effects in the treatment of breast cancer.

Humber CE, et al. Ann Oncol. 2007. 18(3):409-20.
Jeong YI, et al. Arch Pharm Res. 2011. 34(1):159-67.
Hobbs SK, et al. Proc Natl Acad Sci USA. 1998. 95:p. 4607-12.
Trotta F, et al. Expert Opin Drug Deliv. 2014. 11(6):931-41.
Gigliotti CL, et al. J. Biomed. Nanotechnol. 2016. 12: 114-127.
Minelli R, et al. Eur J pharm Sci. 2012 20;47(4): 686-94.
Iezzi M, et al. Translational Animal Models in Drug Discovery and Development. Pp. 139-166 (28).

Corresponding author: Benedetta Ferrara
benedetta.ferrara@unito.it